170–176 Vol. 78 No. 1 ACTA GEOLOGICA SINICA Feb. 2004
http://www.geojournals.cn/dzxbcn/ch/index.aspx

Anchimetamorphism of the Neoproterozoic and the Lower Paleozoic along the Profile of Yuanguping in Western Hunan Province, China

WANG Hejing, CHEN Tao, WANG Huan and ZHANG Zuqing
"Orogene and Crust Evolution" Key Laboratory of the Ministry of Education of China; School of Earth and Space Sciences, Peking University, Beijing 100871; E-mail: hjwang@pku.edu.cn

Abstract The Neoproterozoic and Lower Paleozoic along the profile of Yuanguping in western Hunan Province, China underwent anchimetamorphism. The illite crystallinity (IC) of the <2 μm fractions ranges from 0.23–0.34°Δ2θ for the Neoproterozoic to 0.23–0.35°Δ2θ for the Lower Paleozoic (calibrated with the Kisch IC set, Kisch, 1991). This indicates that the metamorphic grade of the Neoproterozoic and Lower Paleozoic is the anchizone. The peak metamorphic temperature is estimated to be 290–210°C. This result does not agree with the greenschist or subgreenschist facies of the Banxi Group, nor with the lower-greenschist facies or sedimentary cover of the Sinian to Lower Paleozoic, as most previous researchers thought. The illite (K-mica) b_0 values range from 0.9074 to 0.8963 (nm) for the Neoproterozoic and the Lower Paleozoic. Based on cumulative frequency curves of the illite (K-mica) b_0, the peak metamorphic pressure of the Banxi Group was derived to be of a type that is slightly higher than that of the N. New Hampshire low-intermediate pressure type. Most illites occur as the $2M_1$ polytype and some in the Neoproterozoic as a mixture of the $2M_1$+1M types. The distributions of coherent scanning domains (CSDs) of illites along the profile, measured with the XRD method, display a lognormal model and spread out with decreasing Kübler Index of IC. It indicates that illites underwent an Ostwald ripening. The post-anchimetamorphic structural movement not only results in a series of faults but also induces the lattice strain in minerals along the faults and hence impacts the illite crystallinity and causes diagenetic samples to occur within the anchizone. Compared with the cases in eastern and central Hunan Province, the Neoproterozoic and Lower Paleozoic rocks in the west underwent a lower-temperature anchimetamorphism with a pressure lower than that in the east and higher than that in the center of Hunan Province.

Key words: illite crystallinity, polytypism, cell dimension, lattice strain, domain size, anchimetamorphism, Neoproterozoic, Lower Paleozoic

1 Introduction

The Neoproterozoic and the Lower Paleozoic occur along the Yuanguping profile in western Hunan Province, China. There exist two major opinions on the diagenesis and metamorphism around Hunan Province: One (Lu, 1988) considered that the Meso-Neoproterozoic (the Lengjiaxi and Banxi groups) underwent regional low-temperature dynamic metamorphism of lower greenschist facies and reached the sericite-chlorite isograde during the Mesoproterozoic and Neoproterozoic stages and that the Sinian and the Lower Paleozoic underwent regional low-temperature dynamic metamorphism of lower greenschist facies (phyllite) during the Caledonian stage. The other (Jin and Sun, 1997) believed that the regional metamorphism of the Meso-Neoproterozoic in Hunan Province belongs to the isograde of sericite from subgreenschist facies to lower greenschist facies at 200–400°C, while the Sinian to Silurian are the sedimentary cover after the Xuefeng movement (10,000 Ma). The former opinion is based on the analysis of mineral assemblage and the latter on those of authigenic layered mineral assemblages and crystallinity (dimension of fractions). Based on the illite crystallinity (IC, in °Δ2θ, CuKα, hereafter abbreviated as °Δ2θ), polytype and cell dimension, Zhu and Wang (2001) recognized the epimetamorphism and high anchimetamrphism (IC=0.18–0.26°Δ2θ, calibrated with Kisch IC set, 1991) in the Lengjiaxi Group, and high anchimetamrphism (IC=0.21–0.28°Δ2θ) in the Banxi Group in eastern Hunan Province. Wang et al. (2003) concluded from the IC, polytype, cell dimension and lattice strain analyses that the Meso-Neoproterozoic and the Lower Paleozoic in northern-central Hunan Province underwent very low-grade metamorphism (IC= 0.18–0.21°Δ2θ in the Lengjiaxi Group, IC=0.19–0.23°Δ2θ in the Banxi Group and IC=0.20–0.29°Δ2θ in the Sinian to Lower Paleozoic). It is rendered from those data that the grade of metamorphism increases slightly from the east to the center of Hunan Province (Peng et al., 2000). However, the situation in the west requires further study.

The aim of this paper is to study the very low-grade metamorphism and the Neoproterozoic-Lower Paleozoic "sedimentary cover" of western Hunan Province and to reveal the variation of the very low-grade metamorphism from east to west throughout Hunan Province. Besides the mineral assemblages and structural variations of layered silicates, the crystal growth mechanism analysis was also used in this study.

2 Geological Setting

The western part of Hunan Province is tectonically located in the northern-central part of the Jiangnan structural domain of the Yangtze massif (Jin and sun, 1997). The Neoproterozoic consists of a set of clastic-volcanic and deep-sea sediments settled in the Jiangnan domain. In the early Neoproterozoic the Wuling movement took place, followed by folding, lifting and erosion. The Lengjiaxi Group (Pt_2ln) of the Mesoproterozoic occurs under the Wuling unconformity as the oldest stratum in Hunan Province. The Banxi Group of the Neoproterozoic occurs above the Wuling unconformity and disconformitly under the Fulu Formation of the Sinian. The Banxi Group is composed of conglomerates, sandstones, slates, tuffstones and meta-volcanic rocks. The Madiyi Formation (Pt_3bnm) and the Wuqiangxi Formation (Pt_3bnw) compose the lower and higher parts of the Banxi Group. The former consists of a set of yellow-green pelitic and sandy slates and the latter is chiefly composed of quartz sandstones intercalated with slates. The Sinian (Z) is recognized as a platform-type sedimentary cover formed after the Xuefeng orogeny. The sediments of the Sinian are characteristics of cold weather. The main lithologic association includes clastic sandstones containing tillitic-granule, slates, mudstones, dolomites and so on. The Cambrian comprises mainly of limestone, pelitic limestone and marls and characterized by a black carbonaceous slate at bottom. The Ordovician mainly consists of limestone, dolomitic limestone and pelitic limestone. In the study area there is no exposure of the Upper Paleozoic. The Cretaceous occurs in the area as the only Mesozoic stratum lying unconformably over the Paleozoic and Neoprotorozoic (Bureau of Geology and Mineral Resources of Hunan Province, 1988, 1997).

Fifty-eight (58) pelitic rock samples along the Yuanguping profile at sampling intervals of 1 to 3 km were collected. Figure 1 is a geological sketch showing the profile and sampling localities (simplified from the 1:200,000 geological map of Dayong, Regional Geological Surveying Team of the Bureau of Geology and Mineral Resources of Hunan Province, 1969). The profile, starting at E110°32′15″, N29°06′07″ in the north and ending at E110°09′47″, N29°28′36″ in the south, is approximately 39 km long and 8 km from Zhangjiajie City in the north. The samples were collected from the well-exposed outcrops at the sides of the highway.

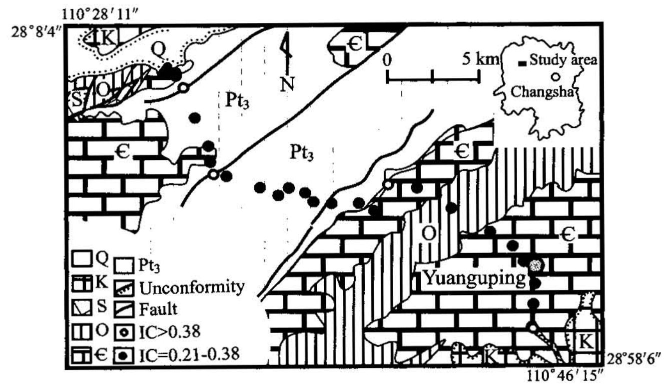

Fig. 1. Geological sketch of the study area, an anchizone, showing localities of profile and samples (modified from the 1:200,000-scale geological map of Dayong, the samples are numbered from south to north corresponding to those listed in Table 1).

3 Methods

About 50 g of rock specimens were crushed with a hammer first and then ground with a DF-4 hammer mill for about 20 seconds. The sedimentation method was used to concentrate the fractions <2 μm, and the suspended liquid was dehydrated with a LXJ-64-1 centrifuge for 30 minutes. Oriented slides were prepared by pipetting suspensions onto glass slides in >3mg/cm^2 and air-dried in room conditions (humidity 20–50%, temperature c. 20°C). The lattice strain was analyzed using the method proposed by Wang and Zhou (2000) and Wang et al. (2002). Analyses of clay coherent domain size were performed by using the software MudMaster (Eberl et al., 1996). All the measurements, conditions and usages were given in Wang et al.'s paper (2003).

4 Results and Discussions

4.1 Mineral phases

Quartz, illite, chlorite and albite are main mineral phases in rocks. Dolomite and calcite are mainly found in the Ordovician, Cambrian and partly in the Neoproterozoic. K-feldspars are found in some Ordovician, Cambrian and Sinian rocks. Some pyrites are found in black slates at the bottom of the Cambrian. It is difficult to recognize the metamorphism from these mineral assemblages and occurrences. All the data including mineral assemblage, illite crystallinity, chlorite crystallinity, illite b_0 values, polytypes and lattice strain are listed in Table 1.

4.2 Illite crystallinity (IC) and chlorite crystallinity (CC)

Illite crystallinity has been used by many researchers for

Table 1 Data of strata, mineral assemblages, IC, CC, b_0, illite polytypes and strains

Sample No.	Stratum	Mineral assemblage	IC (°Δ2*θ*)	CC (°Δ2*θ*)	b_0 (nm)	Illite polytype	τ (%)[a]
HW-133	K_2	Cc, Q, I, Ch, Ab	0.707				
HW-134	Є$_2^2$	Q, Or, I, Ch	0.346	0.219	0.9018	$2M_1$	
HW-135	Є$_3^1$	I, Ch, Q, Or, Ab, Do, Cc	0.246	0.253	0.9010	$2M_1$	
HW-138	Є$_3^1$	I, Ch, Q, Or, Ab, Do, Cc	0.282	0.286	0.9031	$2M_1$	0.2
HW-140	Є$_3^2$	I, Ch, Q, Or, Ab, Do, Cc	0.266	0.261	0.9029	$2M_1$	0.2
HW-141	Є$_3^1$	I, Ch, Q, Or, Ab, Do, Cc	0.241	0.264		$2M_1$	0.286
HW-143	Є$_3^2$	I, Ch, Q, Or, Do, Cc	0.226	0.235	0.9013	$2M_1$	0.16
HW-147	O_1	I, Ch, Q, Or, Ab, Do, Cc	0.248	0.242	0.9034	$2M_1$	
HW-149	Є$_3^3$	I, Ch, Q, Ab, Do, Cc	0.246	0.232	0.9031	$2M_1$	0.245
HW-151	Є$_3^2$	Q, Do, Or, I	0.659		0.8963		out
HW-153	Є$_3^3$	Q, Do, Or, I, Ch, Ab	0.290	0.225	0.9002	$2M_1$	
HW-155	Z	I, Ch, Q, Or, Do	0.344		0.9026	$2M_1$	0.175
HW-157	*Ptbnw*	Q, Ab, I, Ch	0.300	0.311	0.9026	$2M_1$	
HW-158	*Ptbnw*	Do, Q, Ch, I, Cc	0.227				
HW-159	*Ptbnw*	Do, Q, Ch, I, Ab	0.319	0.375	0.9021	$2M_1$+1M	
HW-160	*Ptbnw*	I, Ch, Q, Ab	0.284	0.387	0.9008	$2M_1$+1M	0.23
HW-161	*Ptbnw*	I, Ch, Q, Ab	0.339	0.344	0.9015	$2M_1$+1M	0.26
HW-163	*Ptbnw*	I, Ch, Q, Ab	0.279		0.9034	$2M_1$+1M	0.246
HW-164	Z	I, Ch, Q, Ab	0.292	0.330	0.9015	$2M_1$	0.224
HW-166	Z	I, Ch, Q, Ab	0.308		0.9010	$2M_1$+1M	
HW-169	Z	I, Ch, Q, Or	0.431	0.364	0.9010		0.5
HW-172	Є$_1$	I, Ch, Q, Or, Do, Ab, Py	0.325		0.8992	$2M_1$	0.268
HW-173	Є$_1$	I, Ch, Q, Or, Do, Ab, Py	0.346		0.9010	$2M_1$	
HW-176	Z	Do, Q, I	0.242		0.8963	$2M_1$	
HW-178	Z	I, Q, Ab, Or	0.484		0.8992		Out
HW-179	Є$_1$	Q, Ab, Or, I, , R	0.295		0.9018	$2M_1$	0.165
HW-180	Є$_1$	I, Ch, Q, Ab	0.299		0.9008	$2M_1$	
HW-181	Є$_1$	I, Ch, Q	0.324		0.8989	$2M_1$	0.236
HW-182	Є$_1$	Q, Ab, Cc, I, Ch, Do	0.244	0.219	0.9074	$2M_1$	0.156

Note: Superscript "a" denotes the illite strain in the c* direction, Pr – pyrite, Q – quartz, I – illite, Or – feldspar, Ch – chlorite, Kao – kaolinite, Cc – Calcite, Do – dolomite, Ab – albite. Out: out of the size-strain region.

analyzing the evolution from diagenesis to metamorphism (Frey, 1987; Rahn et al., 1995; Merriman et al., 1995; Mahlmann, 1996; Matenaar et al., 1999; Mullis et al., 2002; Belmar et al., 2002; Carosi et al., 2003). As an important indicator IC is measured from the full width at half maximum (FWHM) of 1 nm XRD reflection of illite. This width in 2 *θ* in CuKα radiation is known as the Kübler Index (Kübler, 1964) and was calibrated with the equation $IC = 1.1823 \times IC_{meas} + 0.052$ for our experimental conditions with the Kisch IC set (Kisch, 1991), which keeps all measurements at an inter-laboratory comparable level. The total variation of IC is from 0.23 to 0.71°Δ2*θ*. The IC value 0.71°Δ2*θ* in the Cretaceous is found to be the maximum, and it is 0.25°Δ2*θ* in the Ordovician. The IC values range from 0.23 to 0.35°Δ2*θ* in the Cambrian and 0.23–0.34°Δ2θ in the Neoproterozoic respectively. It is noted here that three IC values larger than 0.38°Δ2*θ* (belonging to the diagenetic zone) occurring in the northeast fault system were not used and the interpretation will be given in section 4.6. According to the boundaries of anchizone 0.38–0.21°Δ2*θ* (Kisch, 1991), all samples in the Neoproterozoic and the Lower Paleozoic are classified into the anchizone and that from the Cretaceous belongs to the diagenetic zone. The detailed distribution of ICs is given in Table 1.

In this study, 200–300°C was taken as the temperature range for the anchizone (150±50°C as the lower boundary of the anchizone, p. 1, Bucher and Frey, 1994; 300°C as the upper anchizone boundary, p. 293, Kisch, 1987), and the peak metamorphic temperature was estimated as 210-280°C from IC=0.35–0.23°Δ2*θ* with published IC and temperature data (Schmid et al., 1997).

Chlorite crystallinity (CC) is measured from the full width at half maximum of chlorite (002) reflection. It has been reported from several areas that chlorite crystallinity plays a good role as illite crystallinity does (e. g. Antonelli et al., 2003). However, there exists only a weak correlation (IC = 0.4949CC + 0.1468, R^2 = 0.3114, N = 16) between IC and CC in this study and it is consistent with the results of Wang et al. (1996) and Schmidt et al. (1997). Therefore, a further study is needed to understand the effects of various factors on CC .

4.3 The b_0 value of illite

Sassi et al. (1974) and Guidotti et al. (1976) proposed a mica geobarometer and defined three pressure types: b_0<0.9000 nm as a low pressure type, 0.9000 nm <b_0<0.9040 nm as an intermediate pressure type and b_0>0.9040 nm as a high pressure type. As this geobarometer is based on the statistical proportional correlation between the muscovite (mica) b_0 and the pressure of the metamorphic terrene, the usage of the mica geobarometer should be on a basis of statistics. Being a species of the mica group, the illite b_0 has the same meaning as the muscovite b_0 and has been used as a mica b_0 geobarometer by many researchers (Padan, 1982; Yang and Hesse, 1991; Wang, et. al., 1996). The 26 illite b_0 values measured from the Neoprotorzoic to Ordovician range from 0.8963 to 0.9074 nm. As derived from the cumulative frequency curves of these b_0 values, the pressure condition of anchimetamorphism of the Neoprotorzoic to Ordovician is a bit higher than the N. New Hampshire (low-intermediate) pressure type and lower than that of the Lengjiaxi Group (typical intermediate pressure type, Zhu and Wang, 2001) (see Fig. 2).

4.4 The illite polytype

Although there exist some arguments on the role played by the illite polytype to indicate the evolution from diagenesis to metamorphism (Merriman and Roberts, 1985; Frey, 1987; Dong and Peacor, 1996; Merriman and Peacor, 1999), this polytype transformation accompanying the evolution from smectite via I/S to illite has been confirmed by many researches (Yoder and Eugster, 1955; Maxwell and Hower, 1967, Ylagan, 1996). This leads us to consider the illite polytype still as an indicator for the evolution from diagenesis to low-grade metamorphism. Some recent researches consider that there is no intermediate 1M polytype between $1M_d$ and $2M_1$ (Grathoff and Moore, 2002; Bauluz, et al., 2000). However, the identification of the intermediate polytype 1M depends on, to a great degree, the methods used, especially for mixed samples or those with a low content of illite. The XRD method tends to distinguish the polytype on powder average while the SAED (selected area electric diffraction) of TEM focuses on single crystal. The transformation from $1M_d$ to $2M_1$ starts from the late stage of diagenesis or the beginning of metamorphism. There are arguments on when this transformation was finished. It is evidenced by this study that there is the $1M+2M_1$ combination in the stage of anchimetamorphism.

By comparing the difference between the XRD patterns calculated from the JCPDS database (International centre for diffraction data, 1983), polytype and those of (14), (114) and (025) of the these diagnostic reflections of (11), (112) and (023) of the 1M $2M_1$ polytype were used for distinguishing the illite polytype. Our results show that the reflections of (11), (112) and (023) of the 1M mica occur in some Neoproterozoic samples and (14), (114) and (025) reflections of $2M_1$ occur in all specimens (Fig. 3).

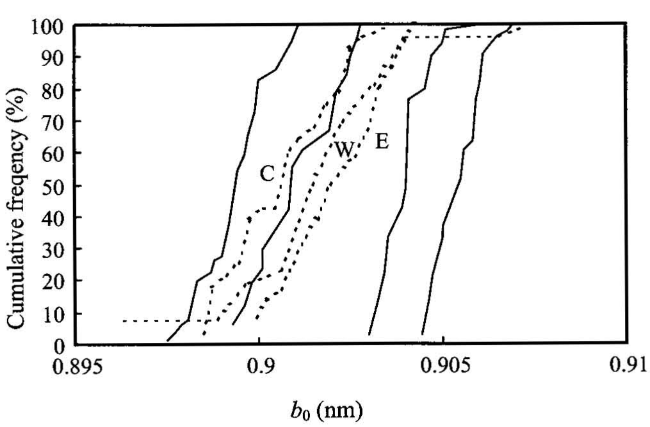

Fig. 2. Cumulative frequency curves of the illite b_0. Solid lines from left to right: the Bosost low pressure type, N. New Hampshire low-intermediate pressure type, Otago intermediate-high pressure type and Sanbagawa high pressure type; dashed lines: W: this study, C: central Hunan, E: eastern Hunan.

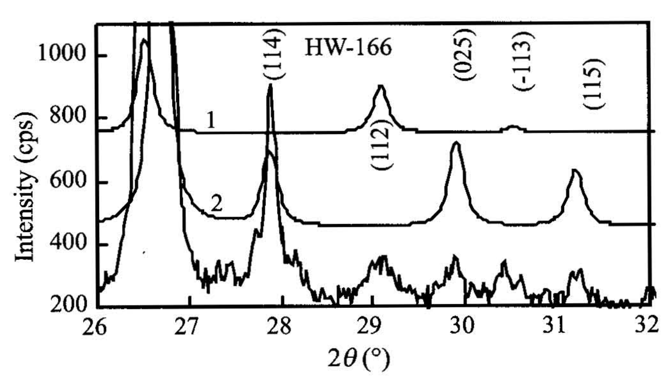

Fig. 3. XRD pattern of illite $1M+2M_1$ polytypes of sample HW-166. Curve 1 is calculated from JCPDS 7-25 (JCPDS, 1983) of 1M polytype and curve 2 from JCPDS 26-911 (JCPDS, 1983) of $2M_1$ polytype. Note that reflection (114) of the illite $2M_1$ polytype coincides with albite reflection (002).

Therefore most illites in rocks from the Neoproterozoic to Ordovician are in the $2M_1$ polytype and only a few in the mixtures of the $2M_1$+1M polytypes. The presence of $2M_1$+1M in the anchizone of the Neoproterozoic is consistent with the conclusion of the IC.

4.5 Particle size distribution and Ostwald ripening

Eberl et al. (1990) published their study result that most clay minerals undergo recrystallization via Ostwald ripening and their particle distribution patterns have a typical lognormal regulation. This has been improved that from nucleation to surface growth mechanism the particle size distribution pattern changes from asymptote to lognormal (Bove et al., 2002; Brime and Eberl, 2002). It is understood from these results that the higher the formation temperature of clay minerals or the higher the diagenetic and metamorphic grade the larger the particle size of clay minerals. Therefore the grain size of clays and their distribution pattern can be used to measure the changes of formation conditions of the clay minerals.

The Bertaut-Warren-Averbach technique (Bertaut, 1950, Warren and Averbach, 1950, software MudMaster, Eberl, et al., 1996) for X-ray diffraction analysis of fundamental particles, the moment calculation (Langford et al., 2000) and the experimental relations between distribution's lognormal parameters (Drits et al., 1997) were used to analyze the mean coherent scattering domain (CSD) of illite. Figure 4 shows that with increasing illite crystallinity (decreasing Kübler Index), the mean coherent domain size and maximum-frequency size generally tend to reach a larger value (crystal growth) while the distribution patterns spread out and the frequency number of particles decreases (lower). This implicates that clay minerals underwent the Ostwald ripening during the anchimetamorphism.

4.6 Lattice strain and its implication

Since lattice strain is an important factor impacting the IC, more and more attention has been paid to the strain effect (Árkai et al., 1997; Jiang et al., 1997; Zulauf et al., 2002). The HW-IR plot (Wang and Zhou, 2000) was used to calculate the lattice strain of some illites in the study area. Since the Weaver Index and the IR are defined from the lower angle side of the illite 1 nm reflection, these peak parameters of HW, As and IR needed in the HW-IR plot (the meanings of the parameters are referred to Wang and Zhou, 2000) were used from the lower angle side of the illite 1 nm reflection. This is different from the previous study of the profile of Huangtudian in northern-central Hunan, which used the HW measured directly from an asymmetric 1 nm peak of illite. The different distortion of asymmetry on the lower and higher angle sides of an XRD peak and the induced difference between the peak parameters on the two sides were neglected in this study. Peaks of low counts with low confidence were not used. As the smoothing technique was not used, some negative Weaver Index or IR data generated from random radiation of X-ray were not used either.

All the lattice strain data range from 16–0.5% and two of them are outside of the higher boundary of the strain domain in the HW-IR plot (Fig. 5). It is generally thought that the higher the stress is the higher the strain will be. The two samples out of the higher boundary of the strain region and the sample with the highest strain value of 0.5% are collected from the northeastern fault belt, which indicates that it is the fault that causes the high strain in the minerals along the fault. That explains why these three daigenetic IC

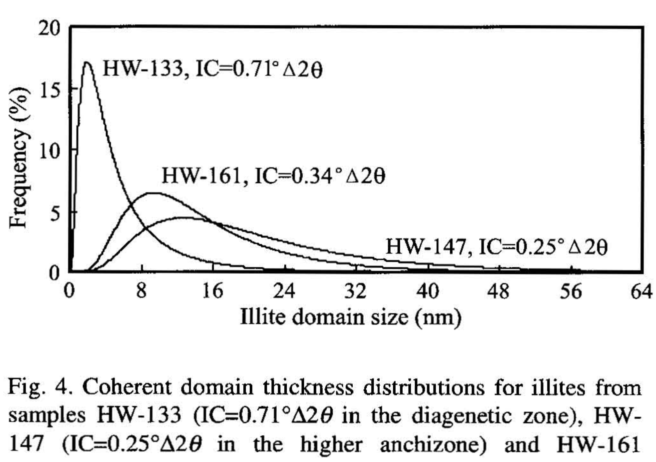

Fig. 4. Coherent domain thickness distributions for illites from samples HW-133 (IC=0.71°Δ2θ in the diagenetic zone), HW-147 (IC=0.25°Δ2θ in the higher anchizone) and HW-161 (IC=0.34°Δ2θ in the lower anchizone).

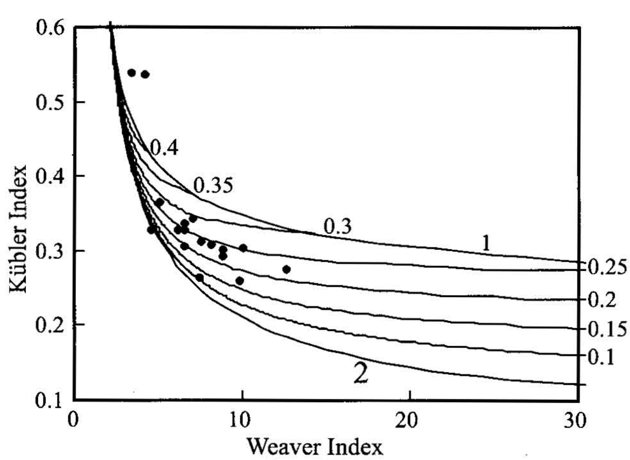

Fig. 5. Lattice strain plotting on the HW-IR plot for illites. Two points out of the size-strain region are from samples HW-178 and HW-169, which were collected from the north-east fault zone. The others filling in the low strain region indicate the relatively low stress effects. Lines 1 and 2 limit the higher and lower boundaries of the size-strain region. The numbers at the ends of other lines mark the values of strain. The asymmetric parameter of the HW-IR plot is set as 2.

values of Kübler Index occur in the anchizone. Other strain data along the Yuanguping profile fall in the range of 0.286–0.16%, which indicates that the stress effects in those area are relatively low.

5 Conclusions

It is concluded from the comparison of this study with that of low-grade metamorphism in eastern and central Hunan that: (1) the rocks of the Neoproterozoic and Lower Paleozoic in western Hunan underwent a lower grade (lower temperature) of anchimetamorphism than that in eastern and central Hunan; (2) the pressure condition in the west is lower than that in the east and higher than in the center of Hunan; (3) during the anchimetamorphism clay minerals underwent an Ostwald ripening and grew up; (4) the post-metamorphic structural movement induced a series of high-grade lattice strains in the minerals along the northeastern fault belt; (5) the illite crystallinity in rocks of the fault belt becomes poorer and hence the Kübler Index of IC grows larger.

Acknowledgments

This work was supported by the National Nature Science Foundation of China (Grant No. 40272022). Thanks are given to Dr. Zhu Yongfeng who reviewed this manuscript and gave good suggestion.

Manuscript received Oct. 28, 2003
accepted Dec. 25, 2003
edited by Zhu Xiling

References

Bureau of Geology and Mineral Resources of Hunan Province, 1988. *Regional Geology of Hunan Province*. Beijing: Geological Publishing House, 9–24 (in Chinese with English abstract).

Bureau of Geology and Mineral Resources of Hunan Province, 1997. *Stratigraphy (Lithostratigraphy) of Hunan Province*. Wuhan: China University of Geosciences Press, 4–122 (in Chinese).

International centre for diffraction data, 1983. *Mineral Powder Diffraction File Databook*, 7–25, 26–911.

Antonelli, F., Zane, A., Sassi, R., Lazzarini, L., and Árkai, P., 2003. Illite Kübler index and chlorite "crystallinity" of marbles as indicators of metamorphic grade. *Geophysical Research Abstracts*, 5: 02142.

Árkai, P., Balogh, K., and Frey, M., 1997. The effects of tectonic strain on crystallinity, apparent mean crystallite size and lattice strain of phyllosilicates in low-temperature metamorphic rocks. A case study from the Glarus overthrust, Switzerland. *Schweiz. Miner. Petrog. Mitt.*, 77: 27–40.

Bauluz, B., Peacor, D.R., and Lopez, J.M.G., 2000. Transmission electron microscopy study of illitization in pelites from the Iberian Range, Spain: Layer-by-layer replacement? *Clays and Clay Minerals*, 48: 374–384.

Belmar, M, Schmidt, S.T., Mahlmann, R.F., Mullis, J., Stern, W. B., and Frey, M., 2002. Diagenesis, low-grade and contact metamorphism in the Triassic-Jurassic of the Vichuquen-Tilicura and Hualane-Gualleco Basins, Coastal Range of Chile. *Schweiz. Miner. Petrog. Mitt.*, 82: 375–392.

Bertaut, M.F., 1950. Raies de Debye-scherrer et repartition des dimensions des domains de Bragg dans les poudres polycristallines. *Acta Crystallogr.*, 3: 14–18 (in French).

Bove, D.J., Eberl, D.D., McCarthy, D.K., and Meeker, G.P., 2002. Characterization and modeling of illite crystal particles and growth mechanisms in a zoned hydrothermal deposit, Lake City, Colorado. *American Mineralogist*, 87: 1546–1556.

Brime, C. and Eberl, D.A., 2002. Growth mechanisms of low-grade illites based on shapes of crystal thickness distributions. *Schweiz. Miner. Petrog. Mitt.*, 82: 203–209.

Bucher, K., and Frey, M., 1994. *Petrogenesis of Metamorphic Rocks* (6th edition). Berlin: Springer-Verlag, 99–146, 191–232.

Carosi, R., Leoni, L., Montomoli, C., and Sartori, F., 2003. Very low-grade metamorphism in the Tuscan Nappe, Northern Apennines, Italy: Relationships between deformation and metamorphic indicators in the La Spezia mega-fold. *Schweiz. Miner. Petrog. Mitt.*, 83: 15–32.

Dong, H., and Peacor, D.R., 1996. TEM observations of coherent stacking relations in smectite, I/S and illite of shales: Evidence for MacEwan crystallites and dominance of $2M_1$ polytypism. *Clays and Clay Minerals*, 44: 257–275.

Drits, V., Srodon, J., and Eberl, D.D., 1997. XRD measurement of mean crystallite thickness of illite and illite/smectite: reappraisal of the Kübler index and the Scherrer equation. *Clays and Clay Minerals*, 45: 461–475.

Eberl, D.D., Drits, V., Srodon, J., and Nüesch, R., 1996. MudMaster: a program for calculating crystallite size distributions and strain from the shapes of X-ray diffraction peaks. *U.S. Geological Survey Open File Report*, 96–171, 55p.

Eberl, D.D., Srodon, J., Kralik, M., Taylor, B., and Peterman, Z.E, 1990. Ostwald ripening of clays and metamorphic minerals. *Science*, 248: 474–477.

Frey, M., 1987. Very low-grade metamorphism of clastic sedimentary rocks, in: Frey, M. (ed.), *Low Temperature Metamorphism*. Glasgaw and London: Blackie, 9–58.

Grathoff, G.H., and Moore, D.M., 2002. Characterization of the Waukesha illite: A mixed-polytype illite in the clay mineral society repository. *American Mineralogist*, 87: 11–12.

Guidotti, C.V., and Sassi, F.P., 1976. Muscovite as a petrogenetic indicator in pelitic schists. *Neues Jahrb. Min. Abhdl.*, 127: 97–142.

Jiang, W.T., Peacor D.R., Arkai P., Toth, M., and Kim, J.W., 1997. TEM and XRD determination of crystallite size and lattice strain as a function of illite crystallinity in pelitic rocks. *J. Metamorph. Geol.*, 15: 267–281.

Jin Wenshan and Sun Dazhong (eds.), 1997. *Texture and Evaluation in Deep Crust of the Continent in the South of China*. Beijing: Geological Publishing House, 4–7, 10–13, 20–22 (in Chinese with English abstract).

Kisch, H.J., 1987. Correlation between indicators of very low-grade metamorphism. In: Frey, M. (ed.), *Low Temperature Metamorphism*. Glasgaw and London: Blackie, 301–304.

Kisch, H.J., 1991. Illite crystallinity: Recommendations on samples preparation, X-ray diffraction settings, and interlaboratory samples. *J. Metamorphic. Geol.*, 9: 665–670.

Kübler, B., 1964. Les argiles, indicateurs de metamorphisme. *Pev. Ftist. Franc. Petro.*, 19: 1093–1112 (in French).

Langford, J.I., Louer, D., and Scardi, P., 2000. Effect of a crystallite size distribution on X-ray diffraction line profiles and whole-powder-pattern fitting. *Journal of Applied Crystallography*, 33: 964–974.

Lu Liangzhao, 1988. The feature of metamorphic rock series of various age and metamorphic megacycles in China. In: Dong Shengbao and Shen Qihan (eds.), *Contributions to Compilation and Study of the Metamorphic Map of China.* Beijing: Geological Publishing House, 1–11 (in Chinese with English abstract).

Mahlmann, R.F., 1996. The pattern of diagenesis and metamorphism by vitrinite reflectance and illite "crystallinity" in Mittelbunden and in the Oberhalbstein. 2. Correlation of coal petrographical and of mineralogical parameters. *Schweiz. Miner. Petrog. Mitt.*, 76: 23–46.

Matenaar, I., Glasmacher, U.A., Pickel, W., Giese, U., Pazukhin, V.N., Kozlov, V.I., Puchkov, V.N., Stroink, L., and Walter, R., 1999. Incipient metamorphism between Ufa and Beloretzk, western fold-and-thrust belt, southern Urals, Russia. *Geol. Rundsch*, 87: 545–560.

Maxwell, D.T., and Hower, J., 1967. High-grade diagenesis and low-grade metamorphism of illite in the Precambrian belts series. *American Mineralogist*, 52: 842–857.

Merriman, R.J., and Peacor, D.R., 1999. Very low-grade metampelites: Mineralogy, microfabrics and measuring reaction progress. In: Frey, M. and Robinson, D. (eds.), *Low Grade Metamorphism.* London: Blackwell, 10–60.

Merriman, R.J., and Roberts B., 1985. A survey of white mica crystallinity and polytypes in pelitic rocks of Snowonia and Llŷn, North Wales. *Mineral. Mag.* 49: 305–319.

Merriman, R.J., Roberts B., Peacor D.R., and Hirons S.R., 1995. Strain-related differences in the crysta-growth of white mica and chlorite—A TEM and XRD study of the development of metamorphic microfabrics in the southern uplands thrust terrane, Scotland. *J. Metamorph. Geol.*, 13: 559–576.

Mullis, J., Rahn, M.K., Schwer, P., de Capitani, C., Stern, W.B., and Frey, M., 2002. Correlation of fluid inclusion temperatures with illite "crystallinity" data and clay mineral chemistry in sedimentary rocks from the external part of the Central Alps. *Schweiz. Miner. Petrog. Mitt.*, 82: 325–340.

Padan, A., Kisch, H.J., and Shagam, R., 1982. Use of the lattice parameter b_0 of dioctahedral illite/muscovite for the characterization of P/T gradients of incipient metamorphism. *Contrib. Mineral. Petrol.*, 79: 85–95.

Peng Jun, Yi Haisheng and Xia Wenjie, 2000. Geochemical indication of Sinian bedded siliceous rocks in the Hunan-Guizhou-Guangxi area and their environmental significance. *Acta Geologica Sinica* (English edition), 74(1): 46–53.

Rahn, M., Mullis, J., Erdelbrock, K., and Frey, M., 1995. Alpine metamorphism in the north Helvetic flysch of the Glarus-Alps, Switzerland. *Eclogae Geol. Helv.*, 88: 157–178.

Sassi, F.P., and Scolai, A., 1974. The b_0 value of the porassie white micas as barometric indicator in low-grade metamorphism of pelitic schists. *Contrib. Mineral. Petrol.*, 45: 148–152.

Schmid, D., Schmid, S.Th., Mullis, J., Mählmann, R.F., and Frey, M., 1997. Very low grade metamorphism of the Taveyanne formation of western Switzerland. *Contrib. Mineral. Petrol.*, 129: 385–403.

Wang, H., Frey, M., and Stern, W.B., 1996. Diagensis and metamorphism of clay minerals in the helvetic Alps of Eastern Switzerland. *Clays and Clay Minerals*, 44: 96–112.

Wang, H. and Zhou, J., 2000. The relationships between the Kübler index, Weaver index and Weber index of illite crystallinity and their applications. *Schweiz. Miner. Petrogr. Mitt.*, 80: 187–198.

Wang Hejing, Lu Anhuai and Chen Tao, 2002. A new method for clay mineral analysis and its application in geology. *Acta Geologica Sinica* (English edition), 76(4): 429–436.

Wang Hejing, Zhou Jian, Xu Qingsheng, Liu Chuxiong and Zhu Mingxin, 2003. Very low-grade metamorphism of the Meso-Neoproterozoic and the Lower Paleozoic along the profile from Huantudian to Xianxi in the central-northern part of Hunan Province, China. *Science in China* (Series D), 46: 672–682.

Warren, B.E., and Averbach, B.L., 1950. The effect of cold-work distortion on X-ray patterns. *J. Applied Phys.*, 21: 595–599.

Yang, C., and Hesse, R., 1991. Clay minerals as indicators of diagenetic and anchimetamorphic grade in an overthrust belt external domain of southern Canadian Appalachinas. *Clay Minerals*, 26: 211–231.

Ylagan, R. F., 1996. Hydrothermal alteration of a rhyolitic hyaloclastite from Ponza Island, Italy. *J. Volcanology Geothermal Research*, 74: 215–231.

Yoder, H.S., and Eugster, H.P., 1955. Synthetic and natural muscovites. *Geochimica et Cosmochimica Acta*, 8: 225–280.

Zhu Mingxin and Wang Hejin, 2001. Very low-grade metamorphism of the Lengjiaxi and Banxi groups around the area of Changsha-Liling-Liuyang, Hunan Province, China. *Acta Petrologica Sinica*, 17: 291–300 (in Chinese with English abstract).

Zulauf, G., Kowalczyk, G., Krahl, J., Petschick, R., and Schwanz, S., 2002. The tectonometamorphic evolution of high-pressure low-temperature metamorphic rocks of eastern Crete, Greece: Constraints from microfabrics, strain, illite crystallinity and paleodifferential stress. *J. Struct. Geol.*, 24: 1805–1828.